

Article

Influence of a Thin V₂O₃ Spacer on Interlayer Interactions in Fe-Ni/V₂O₃/FeNi Film Structures

Gennadiy S. Patrin^{1,2}, Aleksandr V. Kobayakov^{1,2,*}, Vasiliy I. Yushkov^{1,2}, Igor O. Anisimov¹, Sergey M. Zharkov^{1,2} , Sergey V. Semenov^{1,2}  and Evgeniy T. Moiseenko¹

¹ Institute of Engineering Physics and Radio Electronics, Siberian Federal University, 79 Svobodny Pr., 660041 Krasnoyarsk, Russia; patrin@iph.krasn.ru (G.S.P.); viy@iph.krasn.ru (V.I.Y.); igoranisimov98@yandex.ru (I.O.A.); zharkov@iph.krasn.ru (S.M.Z.); svsemenov@iph.krasn.ru (S.V.S.); emoiseenko@sfu-kras.ru (E.T.M.)

² Kirensky Institute of Physics, Federal Research Center KSC Siberian Branch Russian Academy of Sciences, Akademgorodok 50, Building 38, 660036 Krasnoyarsk, Russia

* Correspondence: avk@iph.krasn.ru

Abstract: In this paper, we explore the suggestions of the results of experimental studies on low-dimensional layered systems in FeNi/V₂O₃/FeNi film structures. The multifunctional material V₂O₃ is used as an interlayer between the magnetically active FeNi layers. The films were obtained by ultrahigh vacuum magnetron sputtering on a glass substrate with a base size of 10⁻¹⁰ Torr. It has been found that for V₂O₃ films, the decrease in the metal–semiconductor transition temperature increases significantly. Magnetic characteristics were studied on the MPMS-XL SQUID magnetometer. The exchange effect occurs both in the region where the oxide has a magnetic order and in the paramagnetic region. The latter is due to the effect of the magnetic panel in the oxide package. The phenomenon of oscillation of the exchange field occurs depending on the phenomenon of intermediate observation observed experimentally.

Keywords: ferromagnetic; vanadium oxide; interface anisotropy



Citation: Patrin, G.S.; Kobayakov, A.V.; Yushkov, V.I.; Anisimov, I.O.; Zharkov, S.M.; Semenov, S.V.; Moiseenko, E.T. Influence of a Thin V₂O₃ Spacer on Interlayer Interactions in Fe-Ni/V₂O₃/FeNi Film Structures. *Processes* **2023**, *11*, 2084. <https://doi.org/10.3390/pr11072084>

Academic Editor: Prashant K. Sarswat

Received: 13 June 2023

Revised: 4 July 2023

Accepted: 11 July 2023

Published: 13 July 2023



Copyright: © 2023 by the authors. Licensee MDPI, Basel, Switzerland. This article is an open access article distributed under the terms and conditions of the Creative Commons Attribution (CC BY) license (<https://creativecommons.org/licenses/by/4.0/>).

1. Introduction

Film materials and heterostructures have been paid much attention due to the wide range of properties they possess and the development of technologies for their production. Such systems are then used as building blocks for the fabrication of various advanced technologies, including spintronics devices. In this direction, materials called “multifunctional” become interesting, designed to perform several functions through a reasonable combination of various functionalities. For the direction of spintronics, multifunctional materials are used as sensor elements, magnetic memory elements, etc. [1,2].

For example, for structures in which control elements are based on multifunctional materials, FeBiO₃ and (La,Sr)MnO₃ are widely used: thermistor devices, bolometer-type infrared detectors, multiple-state memory elements and others. In such devices, controlled doping is an effective tool. It can be used, eventually in combination with deformation or other structural distortions, to adapt material properties at the nanoscale [3].

Many properties for film systems are determined by interactions at the interface of various materials [4]. Interfaces change not only the bulk magnetic properties but are also capable of inducing magnetism in non-magnetic layers, changing the nature of the magnetic state. Non-collinearity, interface anisotropy, interface-induced spin textures, etc., occur at the interfaces in heterostructures. The most well-known effects are exchange displacement, magnetic springs, the spin Hall effect and topological insulators. In general, the magnetic characteristics of a material (M_S, T_C, etc.) change whenever its dimensions become comparable to the corresponding magnetic correlation length [5]. Moreover, changes in properties

can be associated with structural changes in the vicinity of the interface, with the thickness of layers or interfacial effects such as mutual diffusion, roughness and deformation.

External electric or magnetic fields, elastic stresses, light irradiation, electric current, etc., can be the methods of controlling properties. In this case, external influences can affect the volumetric properties and/or interfaces. Interfaces play a fundamental role in the development of applied technologies. It has been shown that they can create new types of magnetic states and new means for their rapid manipulation [6]. Most of the research is devoted to films, interfaces and heterostructures based on metals and metal alloys.

Advances in the study of metallic systems have stimulated the study of magnetic heterostructures based on other materials, including semiconductors and oxides, for example [7]. In this regard, structures including layers with a metal–insulator transition (MIT) are of particular interest. Canonical examples of materials in which MIT and structural phase transitions occur are vanadium oxides VO_2 and V_2O_3 . In the VO_2 material, a first-order phase transition occurs at a temperature of about 340 K. In this case, a transition occurs from a dielectric low-temperature phase to a high-temperature metal phase, with a change in resistance up to four orders of magnitude. On the other hand, the transition in the V_2O_3 material occurs at a temperature of about 160 K. In this case, there is a transition from a dielectric antiferromagnetic low-temperature phase to a high-temperature paramagnetic metal phase, with a change in resistance up to five orders of magnitude.

There are many works that have studied the magnetic properties of VO_2/Ni [8,9] and $\text{V}_2\text{O}_3/\text{Ni}$ [10–12] two-layer films and the $\text{Ni}/\text{V}_2\text{O}_3/\text{FeNi}$ [13] spin-valve structure.

In the case of $\text{V}_2\text{O}_3/\text{Ni}$ bilayers, insulating regions appear during a structural transition with decreasing temperature. Due to this small area of Ni, the layer becomes stressed; hence, a decrease in the coercive force is observed below T_c . In addition, the formation of the V_2O_3 layer is likely to occur, and the formation of cell formation between the stressed and weakened portions of the Ni layer is accelerated. During magnetization and demagnetization, this boundary freely acts as a pinning center for the motion of the domain tissue. For samples with lower magnetic roughness, the Ni domains are larger than the V_2O_3 domains. Thus, phase coexistence creates additional magnetic domains, domain walls and pinning in the Ni film [8].

Some work on thin-film vanadium oxide–ferromagnetic structures has shown that interfacial coupling between a ferromagnetic material (Ni, Fe and Co) and vanadium oxide leads to additional strain anisotropy due to the effect of inverse magnetostriction. Therefore, the change in the hysteresis loop of the system due to phase separation strongly depends on the quality of the interface, since there is a coexistence of phases caused by additional pinning of domains at the grain boundaries.

Our work is devoted to the study of interfaces and magnetic properties of a three-layer structure: $\text{FeNi}/\text{V}_2\text{O}_3/\text{FeNi}$ with a metal–insulator transition in V_2O_3 , which is promising as a multifunctional material. Interest in the study of these particular samples is due to the fact that the use of a material as an interlayer between magnetically active layers, which simultaneously has the properties of a metal–semiconductor transition and has a magnetic–paramagnetic transition, opens up new possibilities in the design of structures with desired properties and is practically unexplored. It is important to elucidate the role of the interface between the magnetically active layer and the interlayer in the formation of the magnetic structure, depending on the thickness of the interlayer, the sequence of deposition of layers and the technological conditions for deposition of various layers of the structure. These studies may be important in matters of spin-dependent transport, since the conditions for the injection of spin-polarized electrons, along with the degree of polarization of conduction electrons in magnetic layers, strongly depend on the conjugation of energy bands and scattering processes at interfaces.

2. Materials and Methods

We have tried to study $\text{FeNi}/\text{V}_2\text{O}_3/\text{FeNi}$ three-layer structures with a layer of vanadium oxide V_2O_3 and permalloy (FeNi) magnetic layers.

The films were sputtered onto a glass substrate using an ultrahigh vacuum magnetron sputtering system from Omicron NanoTechnology (Taunusstein, Germany) with Pfeiffer Vacuum turbomolecular pumps. The substrate was placed in the elevator of the working chamber through the sluice system for loading samples. The position of the substrate in the elevator relative to the magnetron was set to 20 cm. The deposition was carried out at a base pressure of 10^{-10} Torr in an argon atmosphere at a pressure of 3 m Torr (with film thickness control system during growth). The substrate was preliminarily cleaned by ion-plasma etching in the working chamber, immediately before the deposition process. All layers were deposited onto a rotating substrate at its temperature $T \approx 373$ K. The vanadium oxide layer was deposited from an AC magnetron using a V_2O_3 target. The permalloy layer was deposited from a DC magnetron using a $Fe_{14}Ni_{86}$ alloy target.

Electron microscopic images and electron microdiffraction patterns are performed using a special JEOL JEM-2100 transmission microscope equipped with an Oxford Inca x-sight energy dispersive spectrometer at a fast voltage of 200 kV (when preparing samples for installing Gatan PIPS). Additional refinement of the layer thicknesses was performed using electron microscopic images. The phase composition was studied by X-ray diffraction analysis (XRD) on a DRON-4-07 instrument (Cu-K α radiation). Analysis of the intensity of diffraction reflections on electron diffraction patterns and their interpretation were made using the Gatan Digital Micrograph software and the ICDD PDF 4+ database.

Magnetic characteristics were studied on the MPMS-XL SQUID magnetometer in fields up to 50 kOe. The measurements were made in the temperature range from 4.2 K to 300 K. The magnetic field lay in the plane of the film. Before each measurement, the film was first placed in a demagnetizer and then cooled in a zero magnetic field (ZFC mode). The four-probe method was used for magnetotransport measurements. The external field was set by an electromagnet when measuring $R(T)$ above 100 K. The external field was perpendicular to the macroscopic transport current ($H \perp I_{macro}$). The critical current was determined by the criterion of $1 \mu V/cm$, and the sample was immersed in liquid nitrogen.

As a result, the following sets of samples were obtained, investigated and analyzed:

1. Three-layer $FeNi/V_2O_3/FeNi$ films with thicknesses $t_{FeNi} \approx 15$ nm, $t_{V_2O_3}$ = from 3 nm up to 19 nm, with a step of 2 nm.
2. In order to study the features of the $V_2O_3/FeNi$ and $FeNi/V_2O_3$ interfaces, two-layer films with different sequences of V_2O_3 and $FeNi$ layers: $SiO_2(substrate)/V_2O_3/FeNi$ and $SiO_2(substrate)/FeNi/V_2O_3$ with thicknesses $t_{FeNi} \approx 15$ nm, $t_{V_2O_3} \approx 30$ nm were obtained.
3. To determine the transition region of vanadium oxide, a series of single-layer V_2O_3 films with thicknesses $t_{V_2O_3} = 20, 30, 40, 50, 80$ and 100 nm was produced.

3. Results

Figure 1a–d show electron microscopic images and electron microdiffraction patterns obtained from cross sections of two-layer $SiO_2(substrate)/V_2O_3/FeNi$ and $SiO_2(substrate)/FeNi/V_2O_3$ films. Interpretation of the diffraction reflexes observed in electron microdiffraction patterns (Figure 1b,d) shows that, regardless of the deposition sequence of the V_2O_3 and $FeNi$ layers, crystalline phases are formed in the films, V_2O_3 having a rhombohedral lattice (spatial R-3c group, lattice parameters: $a = 4.95 \text{ \AA}$, $c = 14.0 \text{ \AA}$, PDF 4+ card #00-034-0187) and an unordered solid solution of Fe-Ni having a cubic face-centered lattice (spatial Fm-3m group, lattice parameter: $a = 3.54 \text{ \AA}$, PDF 4+ card #04-003-2245). The analysis of electron microscopic images suggests that in the case of a $SiO_2(substrate)/V_2O_3/FeNi$ sample (see Figure 1a), the $FeNi/V_2O_3$ interface is more blurred, which indicates a diffusive interpenetration of materials at the interface. In the case of the $SiO_2(substrate)/FeNi/V_2O_3$ sample (see Figure 1c), the $V_2O_3/FeNi$ interface is more pronounced, which indicates the absence of significant materials mixing in the V_2O_3 and $FeNi$ layers. It is natural to expect that such an asymmetry will result in a difference in the physical properties of the $FeNi/V_2O_3$ and $V_2O_3/FeNi$ interfaces.

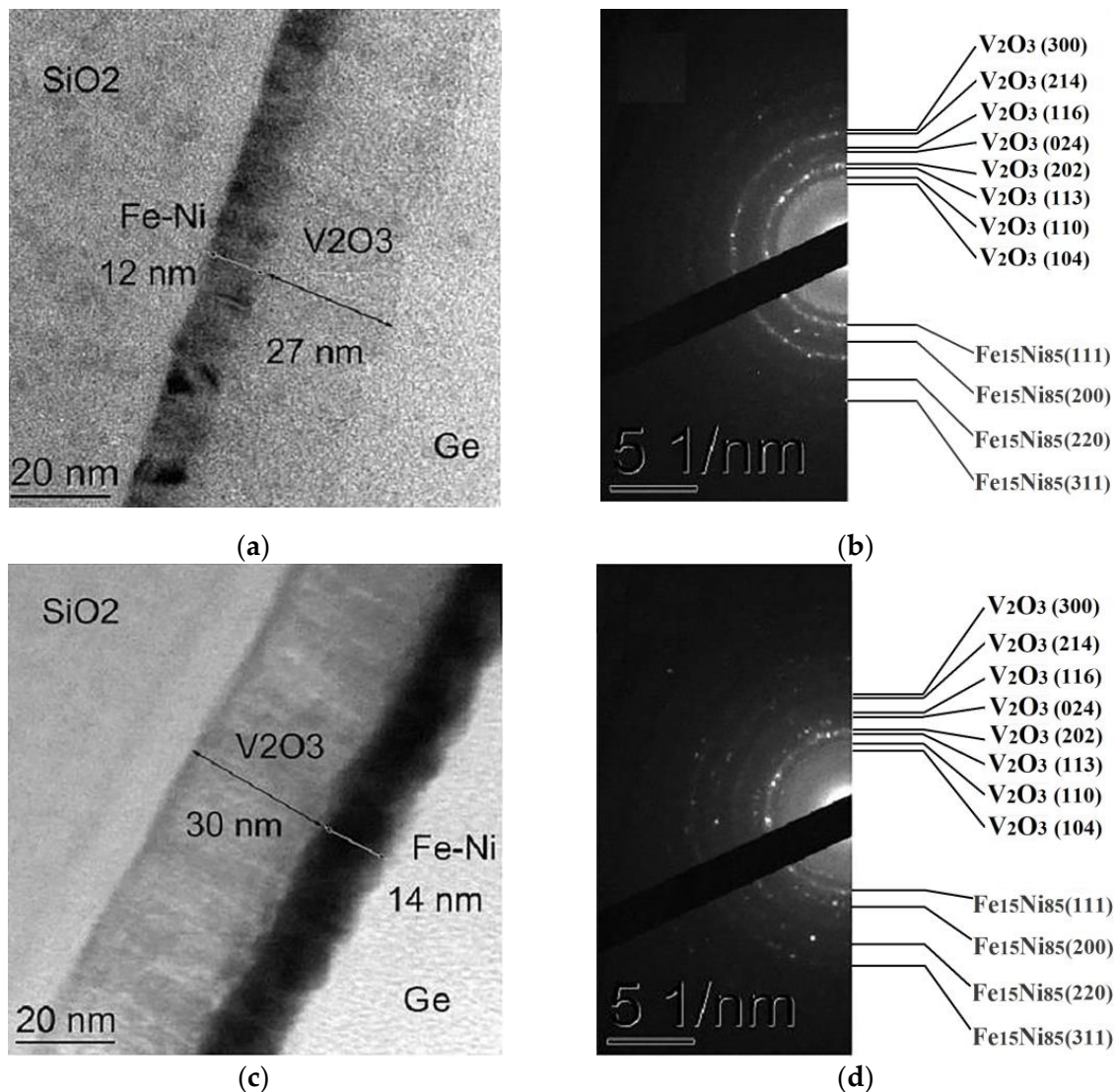


Figure 1. Electron microscopic image (a,c) and electron microdiffraction pattern (b,d) of the cross section. (a,c) SiO₂ film (substrate)/V₂O₃/Fe-Ni; (b,d) SiO₂ film (substrate)/Fe-Ni/V₂O₃.

Figure 2 shows the XRD patterns of the samples: SiO₂ (substrate)/FeNi (50 nm) (a), SiO₂ (substrate)/V₂O₃ (50 nm) (b), SiO₂ (substrate)/V₂O₃ (5 nm)/FeNi (15 nm) (c) and SiO₂ (substrate)/FeNi (15 nm)/V₂O₃ (5 nm)/FeNi (15 nm) (d). The rather thin thicknesses of the film structures make it difficult to obtain better X-ray diffraction patterns of the samples, despite the longer data acquisition times (about five hours or more). However, despite this, the spectra of the film show peaks corresponding to the phases of vanadium oxide V₂O₃ (see Figure 2b–d) and permalloy (FeNi) (see Figure 2a,c,d). Thus, the analysis and interpretation of the X-ray diffraction patterns of the samples show the presence of crystallographic structures corresponding to diffraction reflections obtained from electron microscopic measurements.

It is known [14] that the magnitude and temperature dependence of electrical resistance vary depending on thickness in metal films. Moreover, at small thicknesses for the V₂O₃ composites [15], the temperature behavior of electrical resistance in the vicinity of the metal–insulator transition temperature (T_{MD}) changes depending on the layer thickness and stoichiometry of the material. For bulk crystals of V₂O₃, the value of T_{MD} is 150 K approximately, while at temperatures of $T > 150$ K a paramagnetic state is realized, and below the transition temperature an antiferromagnetic state takes place. Thus, the state

of vanadium oxide (in terms of its electrical resistance) is not unambiguous. Therefore, additional research was carried out to determine this condition.

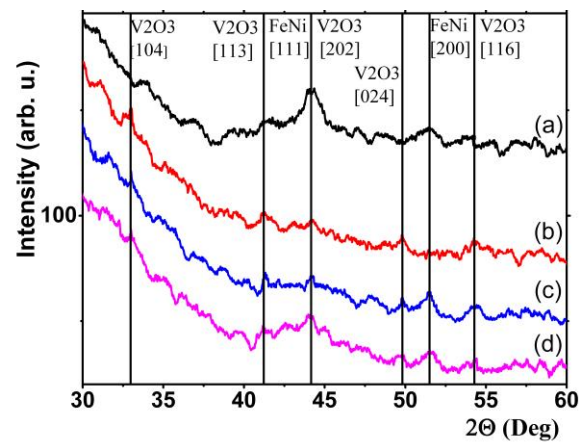


Figure 2. XRD patterns for samples: SiO₂ (substrate)/FeNi (50 nm) (a), SiO₂ (substrate)/V₂O₃ (50 nm) (b), SiO₂ (substrate)/V₂O₃ (5 nm)/FeNi (15 nm) (c) and SiO₂ (substrate)/FeNi (15 nm)/V₂O₃ (5 nm)/FeNi (15 nm) (d).

The curve in Figure 3 represents the experimental temperature dependence of the resistance $R(T)$ of a 30 nm thick V₂O₃ film in the transition region and the T_{MD} determination procedure. The T_{MD} transition temperature is defined as the intersection point of the derivative (dR/dT) with a straight line, which corresponds to the $R(T)$ curve asymptote at the temperature increasing (insert in Figure 3). Thus, the transition temperature MIT corresponds to 191 K for a V₂O₃ film 30 nm thick.

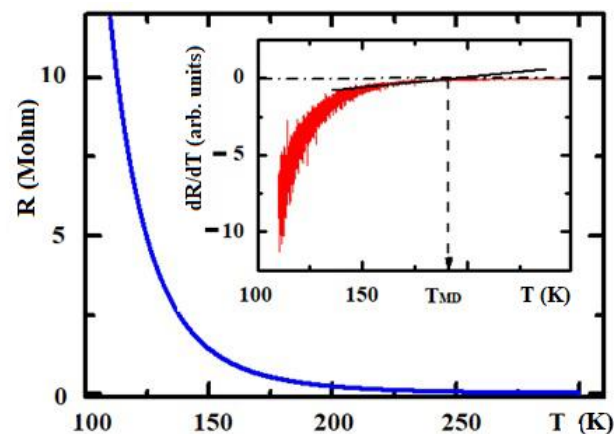


Figure 3. Electron temperature dependence of the film resistance with $t_{V_2O_3} = 30$ nm. The insert shows the temperature dependence of the dR/dT derivative used to determine the transition temperature.

The behavior of the MIT temperature of all obtained single-layer films of the V₂O₃ composites depending on thickness has been studied. The data are shown in Figure 4. It can be seen that at vanadium oxide layer thicknesses of more than 100 nm, the transition temperature practically approaches the transition temperature for a bulk crystal. A sharp increase in the transition temperature takes place when the film thickness decreases less than 50 nm. This result made it possible to determine the maximum thickness of the intermediate layer of vanadium oxide V₂O₃ in the FeNi/V₂O₃/FeNi three-layer composition, at which V₂O₃ can be considered a non-conductive layer for further research.

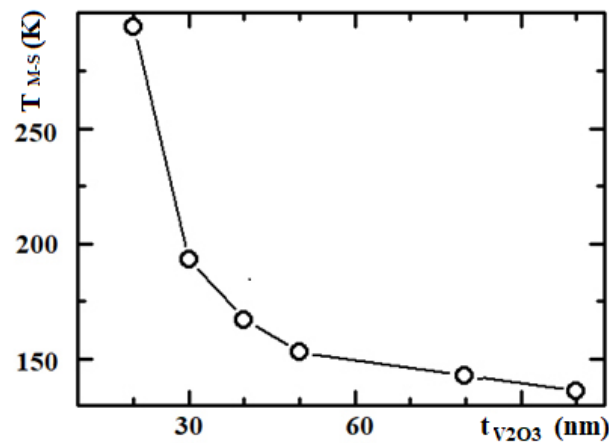


Figure 4. Dependence of the V_2O_3 metal–semiconductor transition temperature on the film thickness.

Below are the results of measurements of the magnetic properties of three-layer systems.

Figure 5 shows the field dependencies of magnetization for FeNi/ V_2O_3 /FeNi films with intermediate layer thicknesses of $t_{V_2O_3} = 3, 7$ and 11 nm (parts a, b and c, respectively), which were taken at different temperatures. It can be seen that the shape of the hysteresis loop depends on the interlayer thickness, while an exchange displacement effect takes place. The presented field dependencies of the magnetization were taken at temperatures $T = 5, 15$ and 75 K.

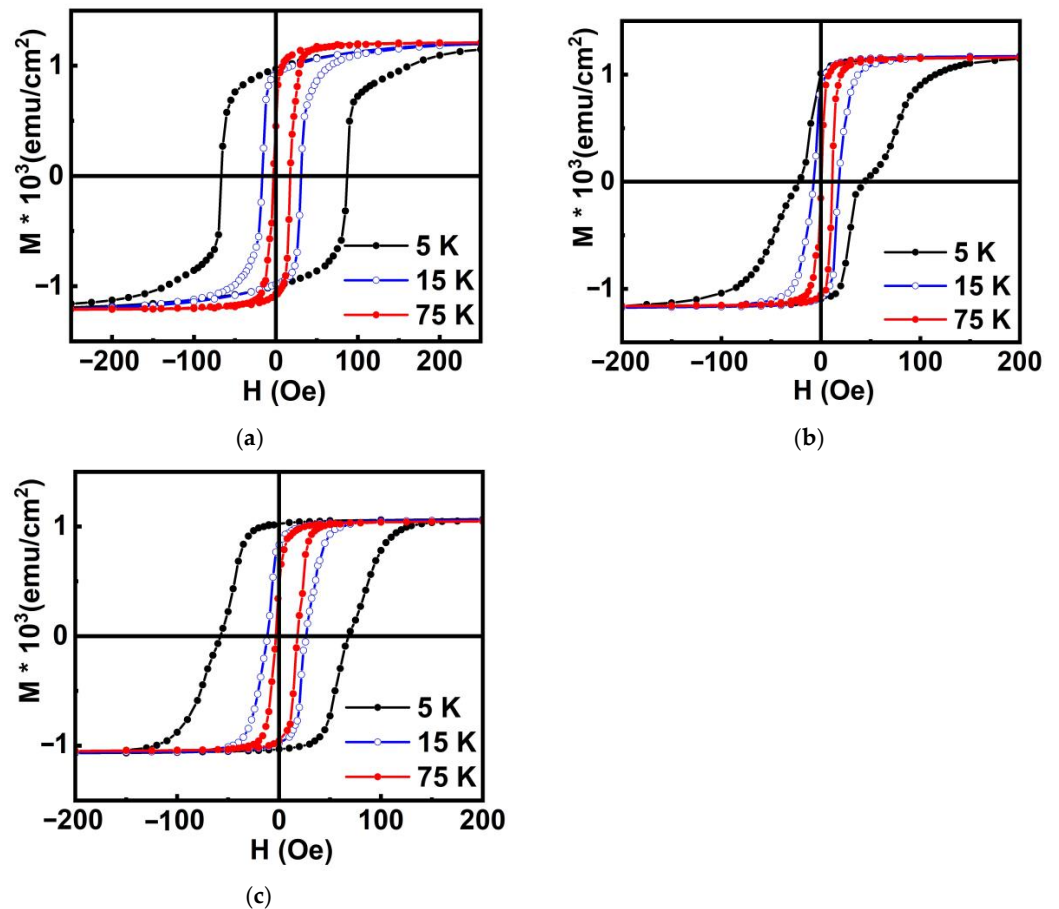


Figure 5. Field dependencies of FeNi/ V_2O_3 /FeNi films magnetization. $t_{V_2O_3} = 3$ (a), 7 (b) and 11 (c) nm. $T = 5, 15$ and 75 K.

The temperature dependencies of the exchange displacement field (H_E) and the coercive force (H_C) of three-layer films are shown in Figure 6 (parts a and b, respectively). Figure 6b shows the dependence at temperatures up to 50 K. Figure 6b shows the dependence of H_C at higher temperatures.

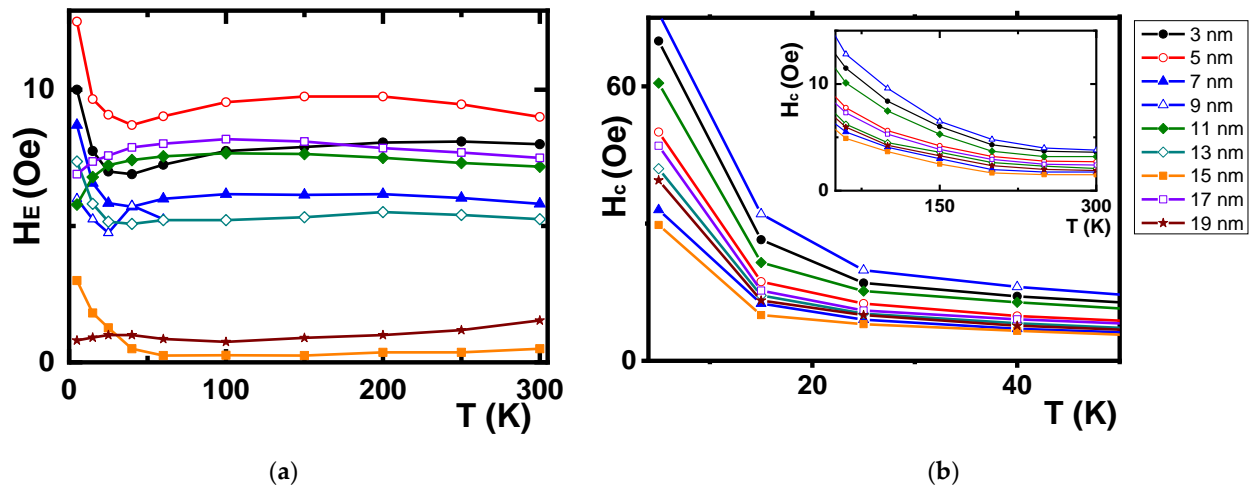


Figure 6. Temperature dependencies of FeNi/ V_2O_3 /FeNi films: (a) exchange displacement (H_E); (b) coercive force (H_C). $t_{V_2O_3} = 3, 5, 7, 9, 11, 13, 15, 17, 19$ nm. The insert shows the H_C dependencies at high temperatures.

All temperature dependencies of the coercive forces demonstrate an increase in the value of H_C with decreasing temperature. In this case, up to a temperature of about 15 K, the value of H_C changes only slightly. Further, the coercive force increases more sharply with decreasing temperature for all thicknesses of the V_2O_3 interlayer. The coercive force of the structure is by one order greater than that of the nominal permalloy layer [16]. Figure 6b also shows that, depending on the thickness of the vanadium oxide layer, H_C oscillations take place. The value of the coercive force decreases from 60 Oe to 15 Oe, with an increase in the thickness of the V_2O_3 interlayer from 3 nm up to 7 nm. Then, the value of the coercive force increases to 45 Oe at the thickness of the V_2O_3 interlayer of 4 nm. Further, as the thickness of the interlayer increases to 15 nm, the coercive force starts to decrease to 8 Oe again.

The curves of the temperature dependencies of exchange displacement fields (Figure 6a) can be divided into two groups according to the nature of behavior in the region of low temperatures during heating.

In the first group of films, the H_E value noticeably decreases with increasing temperature in the range from 4.2 K to 60 K, and then there is a slight increase in the region of $T \approx 150$ –250 K. In the second group of films, the H_E value increases at first to a temperature of about 50 K, and then it reaches a plateau.

In our case, the significant influence of the interlayer on the magnetic properties of ferromagnetic layers (including the values of coercive forces and exchange bias fields) is obvious at temperatures of $T < 40$ K. No changes are observed in the vicinity of the temperature of the proposed electrical transition. The peculiarity of this system is that the effect of exchange displacement is observed in the entire temperature range of measurements, even where no magnetic order in the interlayer V_2O_3 should be. For all films, the sign of the exchange displacement field is positive. As noted above, a state with high electrical resistance is realized throughout the studied area.

4. Discussion

It was previously found [17] that oscillations of the exchange bias field were detected in the Fe/Cr structure, where the authors attribute the observed effect to similar oscillations of the interlayer interaction in Fe/Cr (2 1 1) superlattices. The authors believe that this is

an indication of the linear dependence of the exchange displacement field on the interlayer interaction energy.

The exchange displacement field in the simplest case in two-layer ferromagnetic/antiferromagnetic systems is described by the expression [18]

$$H_E = (\alpha \bullet J_{ex} \bullet |S_F| \bullet |S_{AF}|) / (M_F \bullet t_F) \quad (1)$$

where S_F and S_{AF} are spins in ferromagnetic and antiferromagnetic materials, J_{ex} is the constant of exchange interaction at the interface, M_F and t_F are the magnetization and thickness of the ferromagnetic layer, respectively, and α is the structural factor at the interface. It is known [19] that the effect of positive exchange displacement ($H_E > 0$) is realized in systems (1) when cooling occurs in a negative magnetic field ($h_f < 0$) and positive interlayer interaction ($J_{ex} > 0$) under the condition ($J_{ex} \bullet S_{AF}) < 0$ (with the direction of spin in the antiferromagnet) or in the case (2) when $h_f > |J \bullet S_{AF}|$, but the interlayer exchange is negative ($J < 0$).

Be that as it may, in the evaluation of the flow rate, the structure factor α and the constant interchangeability of J_{ex} at the interface are of interest, given the special multilayer nature of the system. It is realized that, in reality, interfaces are never atomically smooth. Indeed, interface features can be detected in terms of structures, roughness, magnetic properties and domain walls of the ferromagnetic and weakly magnetic layers.

It is known that the deposition of V_2O_3 on permalloy at 750 °C can provoke the appearance of magnetite Fe_3O_4 (111) at the interface, which is the cause of the exchange bias in the Py/ V_2O_3 layers [20]. However, in our case, the skin temperature was lower (373 K). The electron microscopic and X-ray diffraction data do not contain traces of Fe_3O_4 (111) in the films. Therefore, we associate the appearance of the exchange bias with other reasons.

In our case, the cooling of the structure was carried out in a residual magnetic field, when the ferromagnetic layer was in an ordered state, and the V-containing layer was in a paramagnetic state, with a small spin value on the vanadium ion. There, the molecular field of the ferromagnetic layer acts as a cooling field for the vanadium oxide layer. Thus, it is concluded that the exchange between the layers is negative at the beginning of cooling. An exchange displacement in the paramagnetic region of the oxide layer arises due to the fact that in this layer there is a near-surface layer with a magnetic moment other than zero, i.e., there is a bond between the magnetic ions in the permalloy and the V ions at the interface, and the V interphase atoms have an induced magnetic moment.

Such a layer is suggested to arise due to the effect of magnetic proximity, similar to the process in a two-layer V_2O_3/Co system [21]. In this case, the structure of magnetic domains at the interface during magnetization reversal of the ferromagnetic layer controls the effects: fields of the exchange bias, coercive force or blocking temperature. As it is shown in [22], in such systems the exchange is dependent on spatial coordinates, and it decreases with distance from the plane of materials separation and has the form $J \sim \exp(-t/L)$, where L determines the scale of interaction.

Another interesting point is the oscillating dependence of H_C on the thickness of the vanadium-containing layer. For example [23], this behavior is observed in the $LaMnO_3/LaNiO_3$ structure, where $LaMnO_3$ is a ferromagnet and $LaNiO_3$ is a paramagnet, and both have metallic conductivity. Here, according to calculations from the first principles, the resemblance of induced magnetic ordering in $LaNiO_3$ to a spin density wave has been concluded. However, we demonstrate how interlayer interactions can induce a complex magnetic structure in the low-temperature region, in which the V_2O_3 interlayer is not a metal and is in a non-magnetic state.

Initially, a FeNi material with very low anisotropy was used as a ferromagnetic layer, in order to avoid the obscurement of the interactions induced by conjugation with the V_2O_3 layer. As it is known [24], the coercive field is proportional to the anisotropy of the material $H_C = 2 \bullet K / (M_S \bullet \gamma(\theta))$, where, $\gamma(\theta)$ is a parameter depending on the angle θ between the light axis and the direction of the magnetic field; the other designations are traditional.

As it can be seen in Figure 5b, the coercive field decreases rapidly, and changes are very small at temperatures $T > 20$ K. Therefore, the behavior of the coercive force depending on the thickness of the nonmagnetic layer leads to the need to take into account the interface anisotropy.

As a result, the anisotropy at the FeNi/V₂O₃/FeN interfaces may be the sum of one-ion anisotropy of the vanadium ion subsystem and the arising interface anisotropy. According to [25], the constant of one-ion anisotropy (standard designations) is $D = 8.34 \text{ cm}^{-1}$ (≈ 12.07 K), which is consistent in magnitude with the temperature of significant changes in H_C . However, this mechanism alone is not sufficient to explain the behavior of both H_C and H_E at higher temperatures.

All these features in FeNi/V₂O₃/FeNi three-layer films, i.e., an increase in coercivity at low temperature, a positive exchange bias and the presence of coercive force oscillations, are signs of interlayer exchange effects. Apparently, the explanation of such effects in FeNi/V₂O₃/FeNi films is the simultaneous presence of two effects: exchange bias and magnetic proximity.

5. Conclusions

Thus, it has been established in this work that the presence of a V₂O₃ interlayer between permalloy layers leads to a change in the magnetic state. Despite the fact that there should not be magnetic order in the interlayer over the entire temperature range, in this case, the layer has a high electrical resistance.

The main facts and effects found in this study are listed below.

It has been found that the metal–semiconductor transition temperature of the V₂O₃ composites increases strongly at film thicknesses of $t_{V_2O_3} < 50$ nm, and at $t_{V_2O_3} > 100$ nm it tends to the value inherent in the bulk material.

It was found that the V₂O₃/FeNi interface is more pronounced than the interface obtained by reverse deposition of FeNi/V₂O₃ layers under the same conditions. In this case, the presence of crystalline phases does not change, but only diffusion interpenetration of permalloy and vanadium oxide materials occurs at the interface.

It has been found that the shape of the hysteresis loop depends on the thickness of the oxide interlayer.

There is an effect of exchange displacement in the entire temperature range, both in the region of magnetic ordering of vanadium oxide and in the paramagnetic region.

It should be noted that, in general, there are many reports on the change in H_C with temperature for AFM/FM heterostructures, even for similar ones. Our results reflect the behavior of the effect of oscillations of the coercive force depending on the thickness of the interlayer in the FeNi/V₂O₃/FeNi three-layer structure.

The presence of the effect of exchange displacement in the disordered region of vanadium oxide is associated with the effect of magnetic proximity.

These experimental results can be useful for the development of new layered structures for practical applications.

Author Contributions: G.S.P.: conceptualization, methodology, software; A.V.K.: data curation, writing—original draft preparation; V.I.Y.: visualization, investigation; I.O.A.: investigation, validation; S.M.Z.: writing—reviewing and editing, investigation; S.V.S.: investigation, validation; E.T.M.: software, validation. All authors have read and agreed to the published version of the manuscript.

Funding: The research was conducted according to the state assignment of the Ministry of Science and Higher Education of the Russian Federation and the Federal State Autonomous Educational Institution of Higher Education Siberian Federal University (No. FSRZ-2023-0008).

Data Availability Statement: Not applicable.

Acknowledgments: Cross sections of the samples were obtained at the Krasnoyarsk Regional Research Equipment Sharing Center of the FRC KSC Siberian Branch Russian Academy of Sciences and Electron Microscopy Laboratory of the Research Equipment Sharing Center of the Siberian Federal University (RESC SFU). Electron microscopic studies were carried out at the RESC SFU.

Conflicts of Interest: The authors declare no conflict of interest. The funders had no role in the design of the study; in the collection, analyses, or interpretation of data; in the writing of the manuscript; or in the decision to publish the results.

References

1. Lu, C.; Hu, W.; Tian, Y.; Wu, T. Multiferroic oxides thin films and heterostructures. *Appl. Phys. Rev.* **2015**, *2*, 021304. [[CrossRef](#)]
2. Lendlein, A.; Trask, R.S. Multifunctional materials: Concepts, function-structure relationships, knowledge-based design, translational materials research. *Multifunct. Mater.* **2018**, *1*, 010201. [[CrossRef](#)]
3. Ben, H.; Gajek, M.; Bibes, M.; Barthelemy, A. Spintronics with multiferroics. *J. Phys. Condens. Matter.* **2008**, *20*, 434221. [[CrossRef](#)]
4. Hellman, F.; Hoffman, A.; Tserkovnyak, Y.; Beach, G.S.D.; Fullerton, E.E.; Leighton, C.; MacDonald, A.H.; Ralph, D.C.; Arena, D.A.; Durr, H.A.; et al. Interface-induced phenomena in magnetism. *Rev. Mod. Phys.* **2017**, *89*, 025006. [[CrossRef](#)]
5. Vaz, C.A.F.; Bland, J.A.C.; Lauhoff, G. Magnetism in ultrathin film structures. *Rep. Prog. Phys.* **2008**, *71*, 056501. [[CrossRef](#)]
6. Hoffmann, A.; Bader, S.D. Opportunities at the Frontiers of Spintronics. *Phys. Rev. Appl.* **2015**, *4*, 047001. [[CrossRef](#)]
7. Lee, H.-J.; Bordel, C.; Karel, J.; Cooke, D.W.; Charilaou, M.; Hellman, F. Electron-Mediated Ferromagnetic Behavior in CoO/ZnO Multilayers. *Phys. Rev. Lett.* **2013**, *110*, 087206. [[CrossRef](#)]
8. de la Venta, J.; Wang, S.; Ramirez, J.G.; Schuller, I.K. Control of magnetism across metal to insulator transitions. *Appl. Phys. Lett.* **2013**, *102*, 122404. [[CrossRef](#)]
9. Lauzier, J.; Sutton, L.; de la Venta, J. Coercivity enhancement in VO₂/Ni bilayers due to interfacial stress. *J. Appl. Phys.* **2017**, *122*, 173902. [[CrossRef](#)]
10. de la Venta, J.; Wang, S.; Saerbeck, T.; Ramirez, J.G.; Valmianski, I.; Schuller, I.K. Coercivity enhancement in V₂O₃/Ni bilayers driven by nanoscale phase coexistence. *Appl. Phys. Lett.* **2014**, *104*, 062410. [[CrossRef](#)]
11. Urban, C.; Quesada, A.; Saerbeck, T.; Garcia, M.A.; de la Rubia, M.A.; Valmianski, I.; Fernandez, J.F.; Schuller, I.K. Two state coercivity driven by phase coexistence in vanadium sesquioxides/nickel bulk hybrid material. *Appl. Phys. Lett.* **2016**, *109*, 112401. [[CrossRef](#)]
12. Sutton, L.; Lauzier, J.; la Venta, J.D. Magnetic properties of hybrid V₂O₃/Ni composites. *J. Appl. Phys.* **2018**, *123*, 083902. [[CrossRef](#)]
13. Erekhinsky, M.; de la Venta, J.; Schuller, K. Spin valve effect across the metal-insulator transition in V₂O₃. *J. Appl. Phys.* **2013**, *114*, 143901. [[CrossRef](#)]
14. Coffey, K. Electron scattering in metallic thin films. In *Metallic Films for Electronic, Optical and Magnetic Applications. Structure, Processing and Properties*; Barmak, K., Coffey, K., Eds.; Woodhead Publishing Limited: Cambridge, UK, 2014; p. 422. [[CrossRef](#)]
15. Dillemans, L.; Smets, T.; Lieten, R.R.; Menghini, M.; Su, C.-Y.; Locquett, J.-P. Evidence of the metal-insulator transition in unstrained V₂O₃ thin films. *Appl. Phys. Lett.* **2014**, *104*, 071902. [[CrossRef](#)]
16. Patrin, G.S.; Turpanov, I.A.; Yushkov, V.I.; Kobayakov, A.V.; Patrin, K.G.; Yurkin, G.Y.; Zhivaya, Y.A. Effect of the Semiconductor Spacer on Positive Exchange Bias in the CoNi/Si/FeNi Three-Layer Structure. *JETP Lett.* **2019**, *109*, 320. [[CrossRef](#)]
17. Lazar, L.; Jiang, J.S.; Felcher, G.P.; Inomata, A.; Bader, S.D. Oscillatory exchange bias in Fe/Cr double superlattices. *J. Magn. Magn. Mater.* **2001**, *223*, 299–303. [[CrossRef](#)]
18. van der Zaag, P.J.; Ijiri, Y.; Borchers, J.A.; Feiner, L.F.; Wolf, R.M.; Gaines, J.M.; Erwin, R.W.; Verheijen, M.A. Difference between Blocking and Néel Temperatures in the Exchange Biased Fe₃O₄/CoO System. *Phys. Rev. Lett.* **2000**, *84*, 6105. [[CrossRef](#)] [[PubMed](#)]
19. Binek, C. Tunable Exchange Bias Effects. In *Nanoscale Magnetic Materials and Applications*; Liu, J.P., Fullerton, E., Gutfleih, O., Sellmer, D.J., Eds.; Springer: New York, NY, USA, 2009; p. 159. [[CrossRef](#)]
20. de la Venta, J.; Erekhinsky, M.; Wang, S.; West, K.G.; Morales, R.; Schuller, I.K. Exchange bias induced by the Fe₃O₄ Verwey transition. *Phys. Rev. B* **2012**, *85*, 134447. [[CrossRef](#)]
21. Diez, J.M.; Cunado, J.L.F.; Lapa, P.; Arnay, I.; Pedraz, P.; Perna, P.; Bollero, A.; Miranda, R.; Schuller, I.K.; Camarero, J. Interfacial Exchange Phenomena Driven by Ferromagnetic Domains. *Adv. Mater. Interfaces* **2022**, *9*, 2200331. [[CrossRef](#)]
22. Gökemeijer, N.J.; Ambrose, T.; Chien, C.L. Long-Range Exchange Bias across a Spacer Layer. *Phys. Rev. Lett.* **1997**, *79*, 4270. [[CrossRef](#)]
23. Gibert, M.; Zubko, P.; Scherwitzl, R.; Íñiguez, J.; Triscone, J.-M. Exchange bias in LaNiO₃-LaMnO₃ superlattices. *Nat. Mater.* **2012**, *11*, 195. [[CrossRef](#)] [[PubMed](#)]
24. Cullity, B.D.; Graham, C.D. *Introduction to Magnetic Materials*; John Wiley & Sons, Inc.: Hoboken, NJ, USA, 2009; p. 275.
25. Kuwamoto, H.; Robinson, W.R.; Honig, J.M. Magnetic Structure of the Low Temperature Antiferromagnetic Phase of V₂O₃. *J. Sol. St. Chem.* **1978**, *24*, 389. [[CrossRef](#)]

Disclaimer/Publisher's Note: The statements, opinions and data contained in all publications are solely those of the individual author(s) and contributor(s) and not of MDPI and/or the editor(s). MDPI and/or the editor(s) disclaim responsibility for any injury to people or property resulting from any ideas, methods, instructions or products referred to in the content.